RESEARCH ARTICLE OPEN ACCESS

Studying nanotube-based oscillators and their application as memory cells via nanoscale continuum modeling and simulation

Shaoping Xiao*, Weixuan Yang**, Yan Zhang***
*(Department of Mechanical and Industrial Engineering, College of Engineering, The University of Iowa, USA)
** (Product Development & Global Technology Division, Caterpillar Inc., USA)
*** (SMIT Center, School of Mechatronics Engineering and Automation, Shanghai University, China)

ABSTRACT
A nanoscale continuum model of carbon nanotube-based oscillators is proposed in this paper. In the continuum model, the nanotube is discretized via the meshfree particle method. The atomistic interlayer interaction between the outer and inner tubes is approximated by the interlayer interaction between particles. The mechanical behaviors of oscillators are studied and compared well with molecular dynamics simulation results. The nanotube-based oscillator can be employed to design a nanoelectromechanical system. In this system, two electrodes are attached on the top of the outer tube so that the induced electromagnetic force can overcome the interlayer friction. The mechanisms of such nanoelectromechanical systems as memory cells are also considered.
Keywords **-** carbon nanotube, oscillator, memory cell, meshfree, nanoscale continuum modeling

I. INTRODUCTION

Recent developments in nanotechnology promote that nanoscale materials and devices can enhance new engineering techniques in the relevant technology areas, including nanoelectromechanical systems (NEMS). Current advancements in nanotube technology have occurred predominantly in the area of carbon nanotube (CNT) development [1, 2] for nanoscale electronic components and devices [3-7]. Numerical methods play an important role in engineering design to accelerate and foster maturation of nanotechnology that will enable future electronics to become smaller, lighter, multi-functional and autonomous. Since molecular dynamics (MD) has been a powerful tool to elucidate complex physical phenomena at the nanoscale, it is one of the effective candidates to assist nanoengineering designs.

Srivastava [8] proposed a phenomenological design of a single laser-powered molecular motor for CNT-based gears. Using MD simulations, he found that the rotational angular momentum of the driven gear tended to stabilize the rotational dynamics of the system. Kang and Hwang [9] proposed another conceptual design of CNT-based motor. They investigated nanoscale engine schematics composed of a CNT oscillator, motor, channel, and nozzle via MD simulations. Popov et al. [10] reported on three new NEMS designs based on multi-walled carbon nanotubes (MWNT): an electromechanical nanothermometer, a nanorelay, and a nanomotor. They used Ab initio and semi-empirical calculations to estimate the operational characteristics and dimensions of their proposed NEMS systems. Zhao and his co-workers [11] studied CNT devices based on the crossbar architecture and found that this topology was well suited for parallel programming or learning in the context neuromorphic computing.

A few electromechanical models were employed to study CNT-based devices due to the limitation of MD in length and time scales. The electromechanical models can be viewed as continuum models since the electric fields and the configuration of CNTs were modeled via continuum approaches. Axelsson *et al.* [12] presented theoretical and experimental investigations of three-terminal NEMS relays based on suspended CNTs, which were modeled via the classical continuum elasticity theory. Ke and Espinosa [13] examined a switchable CNT-based NEMS with closed-loop feedback. They investigated the pull-in/pull-out and tunneling characteristics of the system by means of an electromechanical analysis, in which the model included the concentration of electrical charge via an empirical function, and the van der Waals force via a continuum approximation. They also used the assumption of continuum mechanics to derive a complete nonlinear equation of the elastic line of the CNT for modeling and simulating CNT-based NEMS devices [14]. In other studies, Bichoutskaia [15] employed an electromechanical model to study interwall interactions in CNTs. Poot *et al.* [16] developed a model for flexural oscillations of suspended CNTs based on the theory of continuum mechanics.

Recently, a few efficient multiscale methods that are capable of addressing large length and time scales have been developed. Multiscale methods either employ a nanoscale continuum approach to approximate a group of atoms [17-19] or couple MD

with continuum mechanics [20-22]. Some researchers have combined the classical MD simulations with the continuum electric models to investigate CNT-based NEMS devices. For example, Kang *et al.* [23] employed this combined method to study suspended CNTs for memory device applications. Dequesnes *et al.* [24] reported a combined MD/continuum simulation of CNT-based NEMS switches. In their research, a multiscale method that combined the nonlinear beam theory with MD was presented to model and simulate CNTs. Xiao and Hou [25] proposed the first numerical modeling and study of CNT-based resonant oscillators. In their multiscale model, the paddle was modeled as the continua while the CNT was modeled via MD. In addition, the molecular and continuum domains were attached with each other at the interfaces via the edge-to-edge coupling [26].

CNT-based oscillators have been of great interest to scientists and engineers since Zheng et al. [27, 28] employed a MWNT to design gigahertz oscillators. A few MD simulations have been conducted to study mechanisms of CNT-based oscillators. The oscillatory frequency of the oscillators might be up to 87 GHz based on MD simulations [29-31]. Legoas *et al.* [29] also pointed out that stable oscillators were only possible when the interlayer distances between the outer and inner tubes were of ~0.34 nm, the interlayer distance of regular MWNTs. Unlike other CNT-based machines, the energy dissipation plays a key role and needs to be considered when designing a stable nano-oscillator. Xiao *et al.* [31] observed mechanical energy dissipation in a CNT-based oscillator, when the oscillator was subject to a finite temperature. Such energy dissipation was found to be strongly dependent on the morphology combination of the tubes [32, 33], and the relative velocity of the inner and outer tubes [34].

As employed in modeling and analysis of many engineering designs, MD has difficulties in simulating large models of CNT-based oscillators. However, the existing continuum approaches and multiscale methods cannot directly be employed. In this paper, we propose a nanoscale continuum model of CNT-based oscillators and study the mechanisms of oscillators as well as their applications as memory cells. Consequently, this research will contribute to assist other engineering design of CNT-based devices.

The outline of this paper is as below. Molecular modeling and simulation of nanotube-based oscillators are reviewed in Section 2. In Section 3, a nanoscale continuum modeling is proposed, and it is employed to study CNT-based oscillators in Section 4. Then, a NEMS design consisting of a nanotube-based oscillator is described and studied as memory cells in Section 5 followed by the conclusion.

II. MOLECULAR MODELING OF CNT-BASED OSCILLATORS

A simple CNT-based oscillator is designed via a double-walled carbon nanotube (DWNT), which consists of an inner tube (core) and an outer tube (shell), as shown in Fig. 1. When the outer tube is partially fixed, the inner tube can oscillate inside the outer tube once it is given an initial velocity or an initial extrusion length.

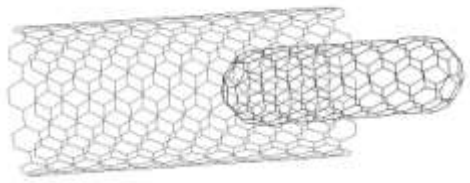

Figure 1. A DWNT-based oscillator.

MD simulations of CNT-based oscillator were conducted [31] via solving the following equations of motion if there were no external forces:

$$m_I \ddot{\mathbf{d}}_I = -\frac{\partial E}{\partial \mathbf{d}_I} = -\frac{\partial \left(E_{inner} + E_{outer} + E_{LJ}\right)}{\partial \mathbf{d}_I} \tag{1}$$

where E is the total potential of the simulated oscillator, which consists of the potential of the inner tube, E_{inner}, the potential of the outer tube, E_{outer}, and the potential due to the interlayer interaction E_{LJ}. m_I is the mass of atom I and $\mathbf{d}_I$ is its displacement.

The reactive empirical bond order (REBO) potential function [35] was used for describing carbon-carbon interatomic interactions within a single CNT. This potential function considers chemical reactions and includes remote effects caused by conjugated bonding, and it can be written as follows:

$$E = \sum_i \sum_{j(>i)} \left[V^R\left(r_{ij}\right) - b_{ij} V^A\left(r_{ij}\right) \right] \tag{2}$$

where r_{ij} is the bond length, $V^R(r)$ and $V^A(r)$ are pair-additive interactions that represent all interatomic repulsions and attractions from valence electrons, respectively. b_{ij} contains the functions that depend on the local coordinates and bond angles for atoms i and j. The detailed formulations of REBO can be found in [35]. The equilibrium carbon-carbon bond length obtained by minimizing this potential is $0.142nm$.

The interlayer interaction between the inner tube and the outer tube is described by the following Lennard-Jones 6-12 potential [36],

$$E_{LJ}(r) = A\left[\frac{1}{2}\frac{y_0^6}{r^{12}} - \frac{1}{r^6}\right] \tag{3}$$

where $A = 2.43\times10^{-24}\,Jnm^6$ and $y_0 = 0.3834nm$. Minimizing the Lennard-Jones potential gives an equilibrium interlayer distance of 0.34nm, which results in stable oscillators as discussed by Legoas and his co-workers [29].

As an example, we consider a (10,10)/(5,5) double-walled nanotube as the oscillator, in which the (5,5) inner tube has a length of 2.5 *nm* while the (10,10) outer tube has a length of 3.7 *nm*. The initial extrusion length is half of the inner tube length. Two MD simulations are conducted. In the first study, the oscillator is considered as an isolated system, i.e. no heat exchanging between the oscillator and its surrounding. The oscillation mechanisms of the oscillator can be studied through the calculated separation distance between the inner and the outer tubes. It is found that the oscillation of the simulated oscillator is stable as shown by the solid line in Fig. 2. The calculated oscillatory frequency is 55 GHz.

In the other simulation, the oscillator is at the room temperature of 300K, and the Hoover thermostat [37] is employed in the MD simulation. As shown by the dashed line in Fig. 2, we find that a stable oscillatory frequency and amplitude cannot be obtained. The oscillatory amplitude decays until the nano-oscillator eventually stops. This phenomenon is caused by the interlayer friction, which mainly dissipates the interlayer energy of the oscillator. Such dissipated energy is transferred to the kinetic energy of the outer tube, and the artificial thermostat thereafter dissipates the energy of the outer tube. As a result, the whole energy of the system is dissipated.

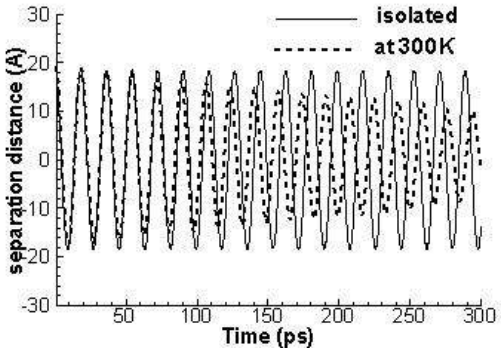

Figure 2. Oscillation mechanism of a (10,10)/(5,5) DWNT-based oscillator.

III. NANOSCALE CONTINUUM MODELING AND SIMULATION OF CNT-BASED OSCILLATORS

III.1 CONTINUUM MODEL OF A SINGLE-WALLED CARBON NANOTUBE

Since a single-walled carbon nanotube (SWNT) can be viewed as an appropriate roll-up of a planar graphene sheet, it is convenient to define the planar graphene sheet as the undeformed or reference configuration during the continuum modeling of a SWNT. The continuum object replacing the crystalline monolayer is a curvature surface without thickness. Therefore, the nuclei are assumed to lie on the surface, and the lattice vectors are chords of the surface.

In most continuum models of nanomaterials, the Cauchy-Born (CB) rule [38] was employed. The Cauchy-Born hypothesis assumes that the lattice vectors deform as line elements within a homogeneous deformation, $\mathbf{a} = \mathbf{F}\mathbf{A}$, where $\mathbf{a}$ and $\mathbf{A}$ are deformed and undeformed lattice vectors respectively. $\mathbf{F}$ is the deformation gradient which maps the "infinitesimal" tangential material vectors of the undeformed body into the vectors of the deformed body. The lattice vectors $\mathbf{a}$ and $\mathbf{A}$, each of which connects two atomic positions, are physical entities with finite length. Consequently, the CB rule holds exactly, at least locally, only when the "infinitesimal" material vector is equivalent to the lattice vector. Therefore, the deformation is assumed to be locally homogeneous.

Arroyo and Belytschko [39] introduced a so-called "exponential Cauchy-Born rule" (ECB rule) to overcome the difficulties of conventional CB rule in approximating curved membranes. The exponential mapping, which maps the lattice vector precisely from the reference configuration to the current one, is approximated locally via the ECB rule based on the stretch and curvature of the membrane. In studying mechanisms of CNT-based co-axial oscillators, we are mainly interested in the longitudinal motion of the CNT. We assume that the nanotube is deformed uniformly in the radial direction so that the out-of-plane motion can be neglected. Consequently, the CB rule is still appropriate as a homogenization technique in the continuum model of SWNTs. In this case, the lattice vectors are approximated in the tangent plane at the material point.

Since only the developable surface with zero Gaussian curvature can be mapped to a planar body, the caps of a CNT, which are semi spheres, cannot be modeled via the proposed continuum approach. However, the need to represent this kind of surfaces can be covered by splitting the surface into pieces. Those pieces can be represented as approximately developable patches, and then glued together with continuity boundary conditions, which are easily accommodated by the Lagrange multiplier technique.

III.2 MESHFREE PARTICLE APPROXIMATION

Using the meshfree particle method [40], the surface of a SWNT is discretized with a number of particles. Since the out-of-plane motion of the nanotube is ignored, the particles are only allowed to move along the surface of the nanotube. It is natural to use the Cartesian components on the planar graphene in Ω^2 to express the particle coordinates in

Ω^3. If we denote $\mathbf{x}$ and $\mathbf{x}_g$ as the Cartesian components of particles in the nanotube and graphene respectively, and *R* as the radius of the nanotube, the mapping can be written as

$$\varphi:\Omega^2 \to \Omega^3 \qquad \mathbf{x}_g \mapsto \mathbf{x} = \varphi(\mathbf{x}_g) \tag{4}$$

or

$$\begin{aligned} x_1 &= R\cos(x_{g1}/R) \\ x_2 &= R\sin(x_{g1}/R), \\ x_3 &= x_{g2} \end{aligned} \tag{5}$$

In a planar graphene sheet, we define $\mathbf{x}_g \in \Omega^2$ in the deformed/current configuration and $\mathbf{X} \in \Omega^2$ in the undeformed/reference configuration. According to the meshfree particle methods [40], the displacement field can be approximated by

$$\mathbf{u}^h(\mathbf{X},t) = \sum_I \omega_I(\mathbf{X})\mathbf{u}_I(t) \tag{6}$$

where $\omega_I(\mathbf{X})$ are called Lagrangian kernel functions. The deformation gradient is then written as $\mathbf{F} = \partial \mathbf{x}_g / \partial \mathbf{X}$, in which $\mathbf{x}_g = \mathbf{X} + \mathbf{u}^h$.

The nominal stress, $\mathbf{P}$, can be computed as

$$\mathbf{P}(\mathbf{F}) = \partial w_C(\mathbf{F}) \Big/ \partial \mathbf{F}^T \tag{7}$$

where w_C is the strain energy density and calculated as the potential density via the CB rule. It should be noted that the free energy density will be employed in equation 7 when considering the temperature effects via the temperature-related Cauchy-Born rule [18].

The internal force in Ω^2 is then calculated as

$$\mathbf{f}_{gI}^{\text{int}} = \int_{\Omega_0} \frac{\partial \omega_I(\mathbf{X})}{\partial \mathbf{X}} \mathbf{P} d\Omega_0 \tag{8}$$

which can be mapped onto the nanotube as

$$\mathbf{f}_I^{\text{int}} = \varphi(\mathbf{f}_{gI}^{\text{int}}) \tag{9}$$

Indeed, the equations of motion solved in Ω^3 are

$$m_I \ddot{\mathbf{u}}_I = \mathbf{f}_I^{ext} - \mathbf{f}_I^{\text{int}} \tag{10}$$

where m_I and $\mathbf{f}_I^{ext}$ are the mass and the external force of particle *I*, respectively.

III.3 NON-BONDED INTERLAYER INTERACTION

The internal forces calculated above are due to the deformation of the nanotube itself. In the MD simulation of CNT-based oscillators, the non-bonded interlayer interaction, as in equation 3, plays an important role. Although a SWNT or single layer of a MWNT can be modeled by the continuum approximation with the meshfree particle method as described in the above, the continuum approach to interlayer interaction, Lennard-Jones interaction, remains an issue. In the meshfree particle method-based continuum model, this issue becomes how to map the Lennard-Jones interaction between two groups of atoms to the interaction between two particles.

To calculate the non-bonded energy in the continuum level, two representative unit cells, one in the inner tube and the other in the outer tube, of area S_0 are chosen. Each of the cells contains *n* nuclei (*n*=2 for graphene). The continuum-level Lennard-Jones energy density is

$$\varphi_{LJ}(d) = (n/S_0)^2 E_{LJ}(d) \tag{11}$$

where $d = \|\mathbf{x}_O - \mathbf{x}_I\|$ is the distance between the centers of those two considered cells.

The total continuum-level non-bonded energy is calculated as

$$\Phi = \int_{\Omega_O}\int_{\Omega_I} \varphi_{LJ}(\|\mathbf{x}_O - \mathbf{x}_I\|) d\Omega_I \, d\Omega_O \tag{12}$$

where Ω_O and Ω_I are the deformed configuration of outer and inner tube respectively. Then, the force applied on particle I can be derived as the first derivative of Φ with respect to the coordinates of particle I. Such forces will be counted as the external forces in solving the following equations of motion,

$$m_I \ddot{\mathbf{u}}_I = \frac{\partial \Phi}{\partial \mathbf{x}_I} - \mathbf{f}_I^{\text{int}} \tag{13}$$

III.3 NANOSCALE CONTINUUM SIMULATIONS

We restudy the oscillation mechanism of the (10, 10)/(5, 5) DWNT-based oscillator as shown in Fig.1 via the meshfree particle method. In the continuum model shown in Fig. 3, the outer tube surface is discretized with 320 particles, and the inner tube is modeled by 152 particles.

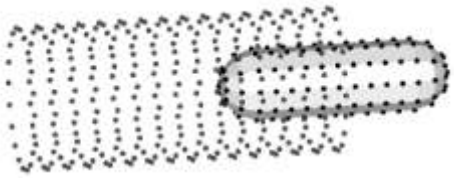

Figure 3. The continuum model of a (10,10)/(5,5) DWNT oscillator.

In the first simulation, the outer tube is fixed and the inner tube is given an initial extrusion, which is half of the inner tube length. When the inner tube is released without any initial velocity, the interlayer force, due to the Lennard-Jones energy between the tubes, will drive the inner tube to move towards the center of the outer tube. The inner tube will be accelerated until the interlayer potential reaches the minimum. The center-of-mass velocity of the inner tube starts to decrease when the interlayer potential increases. Once the center-of-mass velocity of the inner tube becomes zero, the separation reaches the

maximum. Then the interlayer force tends to drive the inner tube backwards to the center of the outer tube. Fig. 4 shows the evolution of separation distance obtained from the meshfree particle method and compared well with the molecular dynamics result. The calculated oscillatory frequency is around 55GHz which agrees to molecular dynamics simulations [31] as well.

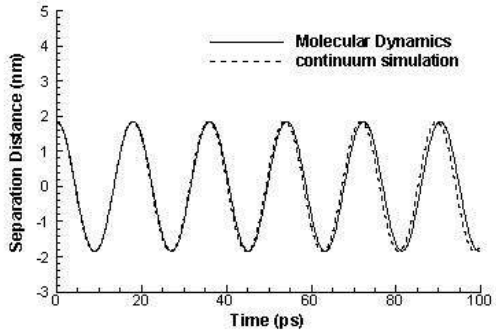

Figure 4. Separation distance evolutions.

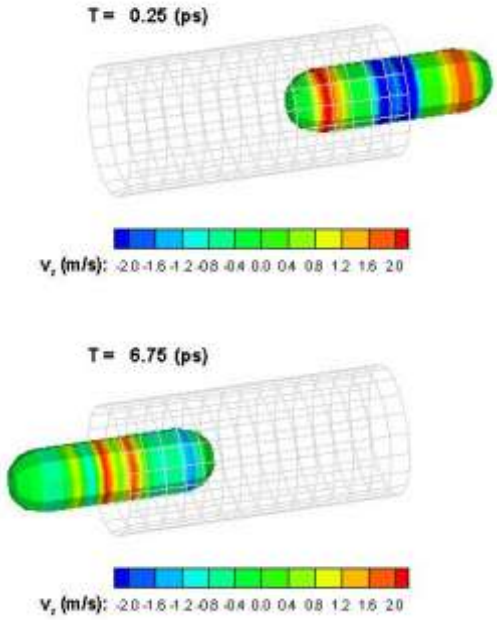

Figure 5. Relative velocity contours on the inner tube at various times.

In this simulation, we observe that shock waves propagate along the inner tube when it oscillates inside the outer tube. Fig. 5 illustrates the relative velocities, which are the particle velocities with respect to the local coordinate system at mass center of the inner tube. It can be seen that several shock waves are generated on the inner tube during its oscillation. Those shock waves propagate back and forth between the ends of the inner tube and interact with each other. However, the relative velocities are very small in comparison with the velocity of the center-of-mass of the inner tube. It should be noted that the background meshes of the outer tube are plotted in Fig. 5 for visualization.

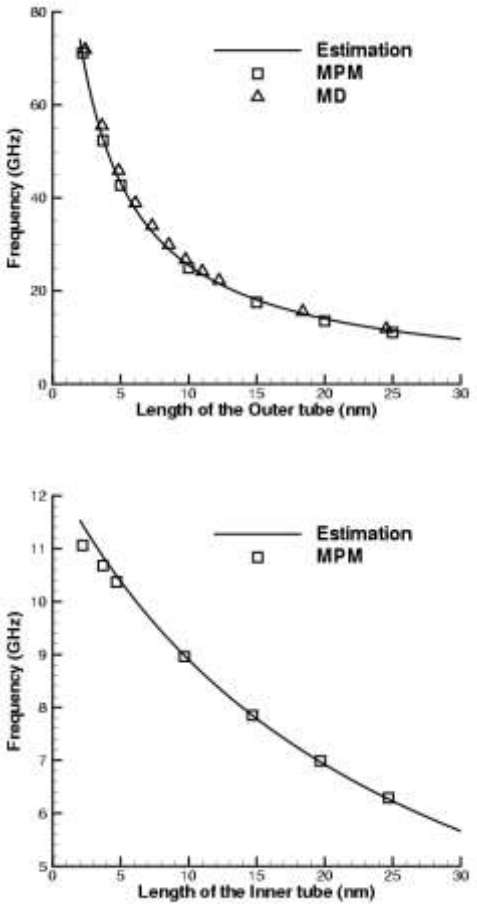

Figure 6. The effects of outer tube length (top) and inner tube length (bottom) on the oscillator frequency.

We also investigate the effect of tube length on the frequency of CNT-based oscillators. We first study (10,10)/(5,5) DWNT-based oscillators with various length of the outer tube. The inner tube has a constant length of 2.5 nm and the initial extrusion is half of its length as described in the above. Fig.6 (top) shows that the oscillatory frequency is lower with a longer outer tube. It agrees well with MD simulations as well as the estimation in [31]. To study the effect of the inner tube length on the frequency of oscillators, we use the (10,10) outer tube with the length of 25 nm. Fig.6 (bottom) concludes that the frequency becomes lower with a longer inner tube.

The interlayer friction was observed in the nano oscillator at a finite temperature via MD simulations [31]. In the nanoscale continuum simulation, the interlayer friction is prescribed as the external force when solving the equations of motion. It has been

shown in [31] that the interlayer friction depends on the temperature as well as the chirality difference of the inner/outer tubes. However, the calculated interlay frictions have the same order as what Cumming and Zettles [41] predicted, i.e. 0.015 pN per atom. In this paper, we mainly study the mechanisms of CNT-based oscillators at the room temperature of 300K, and the interlayer friction of 0.025 pN per atom at the room temperature is employed based on MD simulations. Therefore, the equations of motion, i.e. equation 13, solved in nanoscale continuum simulations are modified as

$$m_I \ddot{\mathbf{u}}_I = \frac{\partial \Phi_{LJ}}{\partial \mathbf{x}_I} - (0.025e - 9)N \frac{v_{Iz}}{|v_{Iz}|}\mathbf{e}_z - \mathbf{f}_I^{\text{int}} \qquad (14)$$

where N is the number of atoms that one particle represents in the nanoscale continuum model.

We restudy the oscillation of the (10,10)/(5,5) DWNT-based oscillator at 300K. The energy dissipation is observed and the oscillation is getting weaker and weaker till ceasing as shown in Fig. 7. It compares well with the MD simulation results in [31].

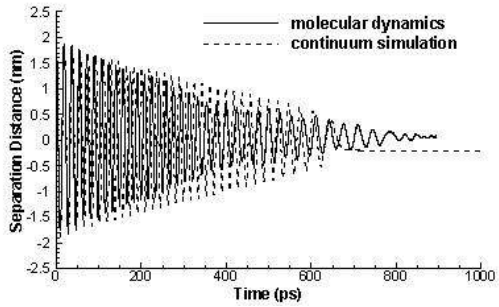

Figure 7. Separation distance evolutions when the oscillator is at the room temperature of 300K.

IV. CNT-BASED MEMORY CELLS

IV.1 A CNT-BASED NEMS SYSTEM

Since the CNT-based oscillator's oscillatory motion is not stable at a finite temperature, a NEMS is designed so that stable oscillation can be achieved. The conceptual idea is shown in Fig. 8. A DWNT is positioned on top of a conducting ground plane. It should be noted that the outer tube is semiconducting while the inner tube can be either metallic or semiconducting. For example, a (17,0)/(5,5) DWNT can be used here since (17,0) CNTs are semiconducting while (5,5) CNTs are metallic. The atomic materials for conducting electrodes 1 and 2 are deposited on top of the outer nanotube. In this configuration, the inner tube sits in a double-bottom electromagnetic potential well. The depth of the potential well under electrode 1 is proportional to the voltage applied to electrode 1. Similarly, the depth of the potential well under electrode 2 is proportional to the voltage applied to electrode 2. The electromagnetic forces exist when applying a high voltage to one electrode while a low voltage is applied to the other electrode. Such electromagnetic forces can overcome the interlayer friction. The high applied voltage is referred to as the WRITE voltage, and the low applied voltage is the READ voltage. Consequently, the inner tube will move from one side to another due to the induced electromagnetic forces, and the stable oscillation could be obtained. In most cases, the outer tube is capped so that the inner tube won't escape if the induced electromagnetic forces are too large.

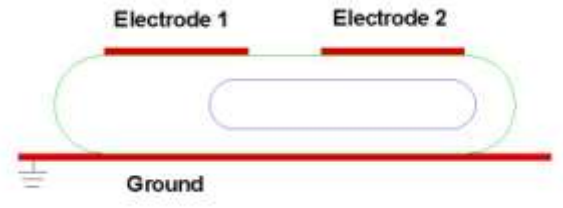

Figure 8. A CNT-based NEMS.

It shall be noted that the capacitance of the NEMS gate can be read by a distinct READ process. A constant-current pulse, i.e. a READ voltage, is applied to one of the electrodes. If the inner CNT is present under that electrode, a relatively large capacitance will be observed, and the time required to charge the electrode will be longer. If the inner tube is not present under that electrode, a relatively small capacitance come forth with a concomitant fast charging time for the electrode. As a result, the logic state of the NEMS gate can be determined. It is worthy to mention that all READ voltages are sufficiently small so that the motion of the inner tube will not be influenced. Whether the inner tube is underneath electrode 1 or electrode 2 will result in two different physical states determined by the READ voltage. These two states can be interpreted as Boolean logic states. Therefore, the system can be used as a random access memory (RAM) cell.

IV.2 COMPUTATIONAL MODEL

The similar nanoscale continuum modeling can be employed to study the proposed CNT-based NEMS. However, the induced electromagnetic forces need to be included as part of external forces when solving the equations of motion.

In the proposed NEMS design, the outer CNT is semiconducting so that its electric property is very similar to that of an insulator. Consisting of two electrodes and the conducting ground plane, the whole device can be viewed as a two-conductor capacitor with the dielectric spaces between them. The capacitance of the system varies with the presence or absence of the inner CNT. In other words, the electric energy stored in the system varies with different positions of the inner tube when a constant voltage is applied on the electrode. Therefore, the inner tube will be driven by the

induced electromechanical force due to the gradient of the electric energy. Poisson's equation is a general way to calculate the electric potential for a given charge distribution, and then the electric field can be obtained

$$\nabla^2\phi = -\rho/\varepsilon_0, \quad \mathbf{E} = -\nabla\phi \tag{15}$$

where ϕ is the potential (in volts), ρ is the charge density (in coulombs per cubic meter), $\varepsilon_0 = 8.854e-12F/m$ is the permittivity of free space (in farads per meter), and $\mathbf{E}$ is the electric field. Then, the capacitance, C, can be expressed as

$$C = \left(\int_S \mathbf{E}\cdot\varepsilon_0 dS\right)\Big/V \tag{16}$$

where S is for a surface integral over the conductor, and V is the potential difference between the electrode and the ground plane.

If the length of the electrode along the longitude direction of the nanotube is sufficiently large as regards with the diameter of the outer nanotube, it can be assumed that the electric field is uniformly distributed along the longitude direction and the fringing regions at the both ends of the electrode are negligible. Here, two cases are considered to calculate the capacitance: the capacitor with or without the presence of the inner tube, respectively. For each case, the electric field and the capacitance can be easily calculated by the two-dimensional model. If the inner tube is partially under the electrode, the system is effectively the combination of two capacitors in parallel, i.e.

$$C = \begin{cases} C_1^t l_0 & \textit{with inner tube} \\ C_0^t l_0 + C_1^t (l_0 - l) & \textit{part of inner tube} \\ C_0^t l_0 & \textit{without inner tube} \end{cases} \tag{17}$$

where C_1^t and C_0^t are the capacitances per unit length with and without inner tube, respectively. l_0 is the inner tube length. l is the length of the inner tube underneath the electrode, and it varies with the positions of the inner tube, i.e. $l = f(z)$. Hence, the induced electromagnetic force applied on the inner tube can be calculated as

$$F(z) = \frac{1}{2}V^2\frac{\partial C}{\partial z} \tag{18}$$

and the equations of motion, equation 14, at the room temperature can be modified as

$$m_I\ddot{\mathbf{u}}_I = \frac{\partial\Phi_{LJ}}{\partial\mathbf{x}_I} - (0.025e-9)N\frac{v_{Iz}}{|v_{Iz}|}\mathbf{e}_z + \frac{1}{2}V^2\frac{\partial C}{\partial z_I}\mathbf{e}_z - \mathbf{f}_I^{\text{int}} \tag{19}$$

Due to the Gauss's law, the calculation of the capacitance should be independent of the potential and the total charge. As an example to calculate the capacitance, a (17,0)/(5,5) DWNT with one electrode of 10V is consider as shown in Fig. 9.

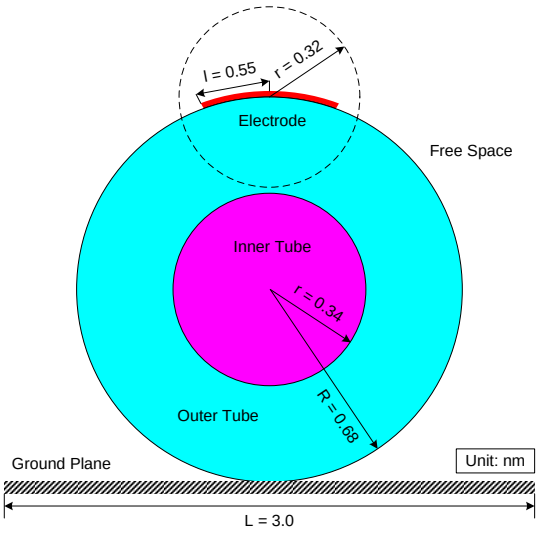

Figure 9. Cross-sectional view of the considered NEMS.

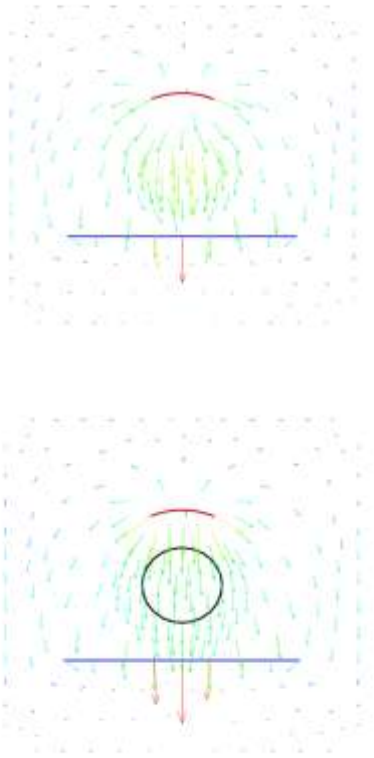

Figure 10. The contours of the electric fields when the inner tube is absent (top) or present (bottom).

Fig. 10 shows the electric fields when the inner tube is absent (top) or present (bottom). The calculated capacitances are $1.03e-19F$ and

$1.11e-19F$, respectively. It should be noted that if the diameter of the outer nanotube is large and the length of the electrode is short, the fringing regions cannot be neglected. In that case, a three-dimensional calculation would be appropriate.

IV.3 SIMULATIONS AND RESULTS

At first, a (17,0)/(5,5) DWNT-based NEMS as the memory cell is considered. In this device, the (17,0) outer CNT has a length of 6.4nm, and the (5,5) inner has a length of 3.7 nm. The electrodes attached to the outer tube are 2.0nm in length and 1.1nm in width. Initially the inner tube is located at the center of the outer tube. In the nanoscale continuum simulations, this device is modeled via 884 particles.

It has been found that the voltage applied on the electrodes cannot be too large; otherwise the CNT could start unraveling carbon chains from the exposed edge. Lee *et al.* [42] claimed that the breakdown voltage of the CNT is round 2.0V/Å. Therefore, the CNTs employed in this NEMS could afford a potential of several hundred volts to maintain its electrochemical stability. Here we apply 16V constant voltage on the two electrodes alternatively with a time interval of 1ns.

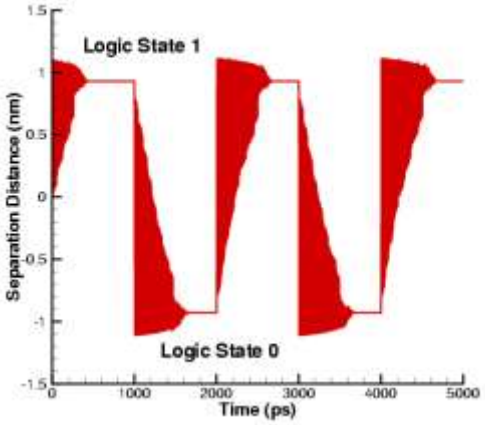

Figure 11: Boolean logic states of the (17,0)/(5,5) CNT-based SRAM cell.

At the beginning, a WRITE voltage is applied on electrode 2. The inner tube is stimulated to move due to the induced electromagnetic force. Such an electromagnetic force overcomes the interlayer friction, and the inner tube moves to be underneath electrode 2. After the inner tube is bounced back by the cap of the outer tube, the interlay friction and the induced electromagnetic force will resist its movement towards to electrode 1. This phenomenon results in the inner tube oscillating underneath electrode 2 till ceasing. The position of the inner tube can be detected by the READ process and the logic state 1 is produced. When the WRITE voltage is shifted to electrode 1, the inner tube moves again and halts under electrode 1. The READ process can detect its position and the logic state 0 is produced as shown in Fig. 11. We also studied CNT-based memory cells with long tubes and observed similar phenomena. It can be seen that the frequency of the memory cell depends on the frequency of the voltage shifting, which means the device working as a SRAM. It can be calculated that the frequency of this SRAM is 500MHz according to the time interval of the WRITE voltage shifting. Fig. 11 also shows that it takes 500ps for the inner tube to cease under an electrode, the recommended maximum frequency is 1GHz.

The proposed memory cell was designed on the basis of the CNT-based oscillator, which has its own natural frequency. The application of the proposed design can be extended to a dynamic random access memory (DRAM) cell if its embedded oscillator can oscillate at its natural frequency. As being studied before, a CNT-based oscillator is an underdamped system, and its oscillation will eventually cease due to the interlay friction when the oscillator is subject to a finite temperature in practical usages. To ensure the oscillator to oscillate consistently at its natural frequency, a WRITE voltage pulse is applied every several oscillation periods to stimulate the oscillator. The period of the WRITE voltage pulse should not be larger than natural period of the oscillator so that the induced voltage acts to enhance oscillation when it becomes weak. Consequently, a steady oscillation can be generated.

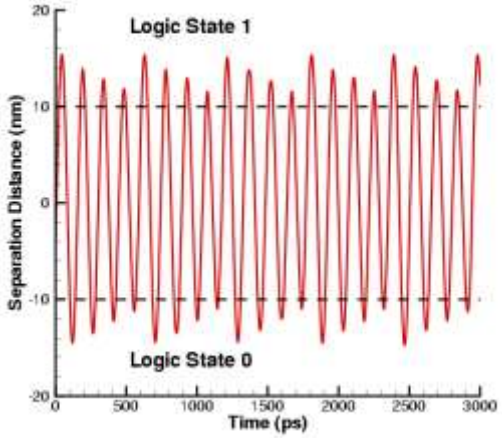

Figure 12. Boolean logic states of the nanotube-based DRAM memory cell.

A memory cell containing a (17,0)/(5,5) CNT-based oscillator as the DRAM is studied here. The (17,0) outer tube has a length of 32 nm while the (5,5) inner tube has a length of 18 nm. The natural oscillating frequency of the oscillator is 6.75 GHz based on the nanoscale continuum simulation. The open-ended outer tube is employed to ensure that the inner tube can oscillate at the natural frequency of the

oscillator. Two 10-nm-long electrodes are attached on the top of the outer tube. A WRITE voltage of 48 V with a duration of 2 ps is applied on electrode 2 so that the inner tube starts to move. Then, the amplitude of the oscillation will decrease due to the interlayer friction. At every four oscillation cycles, the same WRITE voltage pulse is given on electrode 2 to stimulate the oscillation. The WRITE voltage is only applied on electrode 2 in this case to enhance the oscillation from time to time. However, the READ voltage is applied on both electrodes 1 and 2 to generate the logic states 0 and 1 as shown in Fig. 12.

V. CONCLUSION

A nanoscale continuum model was proposed to study the CNT-based oscillators via the meshfree particle method. Both the oscillators as isolate systems and the ones at a finite temperature were studied, and the results agreed well with the MD simulation results. The shock wave propagation and interaction were observed along the inner tube during the oscillatory motion. Since the wave amplitude was small, it didn't have effects on oscillating mechanisms of the oscillator. The proposed numerical model could be referred to as a framework to model and simulate other nanoscale devices.

In addition, a design of NEMS, containing a CNT-based oscillator has been proposed as a memory cell. The electrodes were attached on the top of the outer tube so that the induced electromagnetic force could overcome the interlayer friction when a WRITE voltage was applied on the electrode. On the other hand, a READ voltage was applied to detect the position of the inner tube so that the Boolean logic states could be generated. Numerical simulations showed that the designed NEMS could be employed as either SRAM or DRAM cells.

VI. Acknowledgements

Zhang acknowledges support from NSFC (11272192).

REFERENCES

[1] S. Iijima, Helical microtubules of graphitic carbon, *Nature*, *354*, 1991 56-58.

[2] V. N. Popov, Carbon nanotubes: properties and application , *Materials Science and Engineering R – Reports*, *43(3)*, 2004, 61-102.

[3] P. H. Li, W. J. Zhang, Q. F. Zhang, and J. L. Wu, Nanoelectronic logic circuits with carbon nanotube transistors, *ACTA Physica Sinica*, *56(2)*, 2007, 1054-1060.

[4] Y. A. Tarakanov, and J. M. Kinaret, A carbon nanotube field effect transistor with a suspend nanotube gate, *Nano Letters*, *7(8)*, 2007, 2291-2294.

[5] Y. E. Lozovik, A. G. Nikolaev, and A. M. Popov, Nanotube-based nanoelectromechanical systems, *Journal of Experimental and Theoretical Physics, 103(3)*, 2006, 449-462.

[6] J. Del Nero, F. M. de Souza, R. B. Capaz, Molecular electronics devices: a short review, *Journal of Computational and Theoretical Nanoscience*, *7(3)*, 2010, 503-516.

[7] A. D. Franklin, R. A. Sayer, T. D. Sands, D. B. Janes, and T. S. Fisher, Vertical carbon nanotube devices with nanoscale lengths controlled without lithography, *IEEE Transactions on Nanotechnology*, *8(4)*, 2009, 469-476.

[8] D. Srivastava, A phenomenological model of the rotation dynamics of carbon nanotube gears with laser electric fields, *nanotechnology*, *8*, 1997, 186-192.

[9] J. W. Kang and H. J. Hwang, Nanoscale carbon nanotube motor schematics and simulations for micro-electro-mechanical machines, *Nanotechnology*, *15*, 2004, 1633-1638.

[10] A. M. Popov, E. Bichoutskaia, Y. E. Lozovik, and A. S. Kulish, Nanoelectromechanical systems based on multi-walled nanotubes: nanothermometer, nanorelay, and nanoactuator, *Physica Status Solidi A – Applications and Materials Science*, *204(6)*, 2007, 1911-1917.

[11] W. S. Zhao, G. Agnus, V. Derycke, A. Filoramo, J. P. Bourgoin, and C. Gamrat, Nanotube devices based crossbar artchitecture: toward neuromorphic computing, *Nanotechnology*, *21(17)*, 2010, 175202.

[12] S. Axelsson, E. E. B. Campbell, L. M. Jonsson, J. Kinaret, S. W. Lee, Y. W. Park, and M. Sveningsson, Theoretical and experimental investigations of three-terminal carbon nanotube relays, *New Journal of Physics*, *7*, 2005, 245.

[13] C. H. Ke and H. D. Espinosa, Feedback controlled nanocantilever device, *Applied Physics Letters*, *85(4)*, 2004, 681-683.

[14] C. H. Ke, H. D. Espinosa, N. Pugno, Numerical analysis of nanotube based NEMS devices – Part II: Role of finite kinetics, stretching and charge concentrations, *Journal of Applied Mechanics – Transactions of the ASME*, *72(5)*, 2005, 726-731.

[15] E. Bichoutskaia, Modelling interwall interactions in carbon nanotubes: fundamentals and device applications,

Philosophical Transactions of the Royal Society, *365*, 2007, 2893-2906.

[16] M. Poot, B. Witkamp, M. A. Otte, and H. S. J. van der Zant, Modelling suspended carbon nanotube resonators, *Physica Status Solidi B – Basic Solid State Physics*, *244(11)*, 2007, 4252-4256.

[17] J. Marian, G. Venturini, B. L. Hansen, J. Knap, M. Ortiz, and G. H. Campbell, Finite-temperature extension of the quasicontinuum method using Langevin dynamics: entropy losses and analysis of errors, *Modelling and Simulation in Materials Science and Engineering*, *18(1)*, 2010, 015003.

[18] S. P. Xiao and W. X. Yang, A temperature-related homogenization technique and its implementation in the meshfree particle method for nanoscale simulations, *International Journal for Numerical methods in Engineering*, *69(10)*, 2007, 2099-2125.

[19] S. Q. Chen, W. N. E and C. W. Shu, The heterogeneous multiscale method based on the discontinuous Galerkin method for hyperbolic and parabolic problems, *Multiscale modeling and simulation*, *3(4)*, 2005, 871-894.

[20] N. Choly, G. Lu, W. E and E. Kaxiras, Multiscale simulations in simple metals: A density-functional-based methodology, *Physical Review B*, *71(9)*, 2005, 094101.

[21] G. J. Wagner and W. K. Liu, Coupling of atomic and continuum simulations using a bridging scale decomposition, *Journal of Computational Physics*, *190*, 2003, 249-274.

[22] S. P. Xiao and T. Belytschko, A bridging domain method for coupling continua with molecular dynamics, *Computer Methods in Applied Mechanics and Engineering*, *193*, 2004, 1645-1669.

[23] J. W. Kang, S. C. Kong, H. J. Hwang, Electromechanical analysis of suspended carbon nanotubes for memory applications, *Nanotechnology*, *17*, 2006, 2127-2134.

[24] M. Dequesnes, Z. Tang, and N. R. Aluru, Static and dynamic analysis of carbon nanotube-based switches, *Transactions of the ASME*, *126*, 2004, 230-237.

[25] S. P. Xiao and W. Y. Hou, Studies of nanotube-based resonant oscillators via multiscale modeling and simulation, *Physical Review B*, *75*, 2007, 125414.

[26] T. Belytschko and S. P. Xiao, Coupling methods for continuum model with molecular model, *International Journal for Multiscale Computational Engineering*, *1(1)*, 2003, 115-126.

[27] Q. S. Zheng and Q. Jiang, Multiwalled carbon nanotubes as gigahertz oscillators, *Physical Review Letters*, *88(4)*, 2002, 045503.

[28] Q. S. Zheng, J. Z. Liu and Q. Jiang, Excess van der Waals interaction energy of a multiwalled carbon nanotube with an extruded core and the induced core oscillation, *Physical Review B*, *65*, 2002, 245409.

[29] S. B. Legoas, V. R. Coluci, S. F. Braga, P. Z. Coura, S. O. Dantas, and D. S. Galvao, Molecular-dynamics simulations of carbon nanotubes as gigahertz oscillators, *Physical Review Letters*, *90(5)*, 2003, 055504.

[30] S. B. Legoas, V. R. Coluci, S. F. Braga, P. Z. Coura, S. O. Dantas and D. S. Galvao, Gigahertz nanomechanical oscillators based on carbon nanotubes, *Nanotechnology*, *15*, 2004, S184-S189.

[31] S. P. Xiao, D. R. Andersen, R. Han and W. Y. Hou, Studies of carbon nanotube-based oscillators using molecular dynamics, *International Journal of Computational and Theoretical Nanoscience*, *3*, 2006, 142-147.

[32] W. L. Guo, Y. F. Guo, H. J. Gao, Q. S. Zheng, and W. Y. Zhong, Energy dissipation in gigahertz oscillators from multiwalled carbon nonotubes, *Physical Review Letters*, *91(12)*, 2003, 125501.

[33] J. L. Rivera, C. McCabe and P. T. Cummings, The oscillatory damped behavior of incommensurate double-walled carbon nanotubes, *Nanotechnology*, *16(2)*, 2005, 186-198.

[34] P. Tangney, S. G. Louie and M. L. Cohen, Dynamic sliding friction between concentric carbon nanotubes, *Physical Review Letters*, *93(6)*, 2004, 065503.

[35] D. W. Brenner, O. A. Shenderova, J. A. Harrison, S. J. Stuart, B. Ni and S. B. Sinnott, A second-generation reactive empirical bond order (REBO) potential energy expression for hydrocarbons, *Journal of Physics: Condensed Matter*, *14*, 2002, 783-802.

[36] L. A. Girifalco, R. A. Lad, Energy of cohesion, compressibility and the potential energy functions of the graphite system, *Journal of Chemical Physics*, *25(4)*, 1956, 693-697.

[37] W. G. Hoover, Canonical dynamics - Equilibrium phase-space distributions, *Physical Review A*, *31*, 1985, 1695-1697.

[38] J. Ericksen, The Cauchy and Born hypotheses for crystals, In M. E. Curtin (Ed.), *Phase transformations and material instabilities in solids*, (Academic Press,

1984) 61-77.

[39] M. Arroyo and T. Belytschko, A finite deformation membrane based on inter-atomic potentials for the transverse mechanics of nanotubes. *Mechanics of Materials, 35*, 2003, 193-215.

[40] S. P. Xiao and W. X. Yang, A temperature-related homogenization technique and its implementation in the meshfree particle method for nanoscale simulations, *International Journal for Numerical Methods in Engineering*, *69*, 2007, 2099-2125.

[41] J. Cumings and A. Zettl, Low-friction nanoscale linear bearing realized from multiwall carbon nanotubes, *Science, 289*, 2000, 602.

[42] Y. H. Lee, S. G. Kim and D. Tomanek, Field-induced unraveling of carbon nanotubes, *Chemical Physics Letters, 265*, 1997, 667-672.